REPORT No. 729

TEST OF A SINGLE-STAGE AXIAL-FLOW FAN

By E. Barton Bell

SUMMARY

A single-stage axial fan was built and tested in the shop of the propeller-research tunnel of the NACA. The fan comprised a single 24-blade rotor having a diameter of 21 inches and a solidity of 0.86 and a set of 37 contravanes having a solidity of 1.33. The rotor was driven by a 25-horsepower motor capable of rotating at a speed of 3600 rpm. The fan was tested for volume, pressure, and efficiency over a range of delivery pressures and volumes for a wide range of contravane and blade-angle settings.

The test results are presented in chart form in terms of nondimensional units in order that similar fans may be accurately designed with a minimum of effort. The maximum efficiency (88 percent) was obtained by the fan at a blade angle of 30° and a contravane angle of 70°. An efficiency of 80 percent was obtained by the fan with the contravanes removed.

INTRODUCTION

In connection with tests of airplane cooling systems that are being conducted in the propeller-research tunnel of the National Advisory Committee for Aeronautics, the need was felt for information on axial-fan design inasmuch as the indications are that such fans will be used in airplane cooling systems in the immediate future. In designs of aircraft with submerged engines, it may become necessary to provide a fan that will furnish the necessary volume of air to cool the engines, the oil coolers, and the intercoolers. In pusher-propeller radial-engine installations, the use of an axial fan may help to solve an otherwise difficult cooling problem. The decision was therefore made to build an axial-flow fan with adjustable blades and contravanes and to conduct a series of performance tests on it. The results of these tests are described herein, and the data may be used as a basis for preliminary design studies of superchargers of the axial-fan type.

These data are limited to the characteristics of one particular fan tested over a range of blade and contravane settings. No information is given on the effect of such variables as solidity of blades and contravanes, Mach number, staging for higher pressures, or use of various airfoil sections.

Since the issuance of this report in preliminary form, errors of from 3 to 10 percent were discovered in the pressure and efficiency curves. This error was due to rotation of the air inside the space downstream of the fan hub and affected the reading of the pressure p_c. A slight alteration to the test set-up corrected this source of error. The tests were then repeated and the corrected data are inserted in this report.

DESCRIPTION OF APPARATUS

The single-stage axial-flow fan was built to be used primarily in cooling and duct studies; consequently, an attempt was made to obtain as high a combination of pressure and volume as was consistent with the limitations imposed by the motor power and the fan diameter. Preliminary computations indicated that a volume of 9000 cubic feet per minute at a pressure of 78 pounds per square foot could be obtained. This condition corresponds to 21.2 horsepower. The values in terms of nondimensional quantity and pressure coefficients are $Q/nD^3=0.446$ and $C_p=0.298$ with the fan rotating at a speed of 3600 rpm.

The general arrangement of the blower and the test set-up are shown in figures 1, 2, and 3.

The rotor assembly is shown in figure 4. Attached to the rotor hub are 24 blades that give a solidity of 0.86, the solidity being defined as the result of blade chord times blade length times number of blades divided by disk area. The disk area is the area swept by the blades. Figure 5 is a sketch of an individual blade. Each blade is of R. A. F. 6 section and has a maximum thickness of 12 percent of the chord. Each

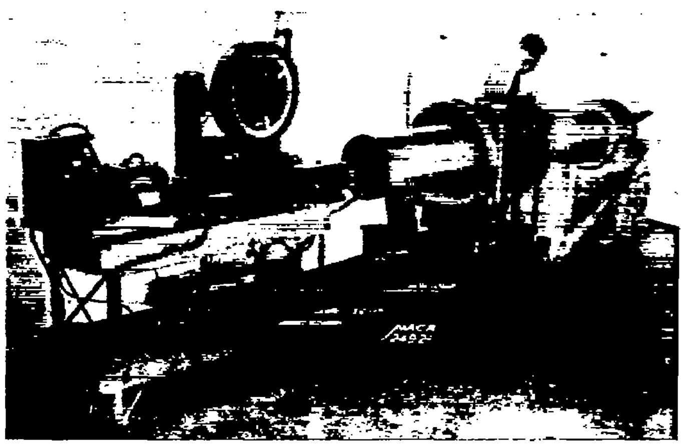

FIGURE 1.—View of axial-fan arrangement from entrance end.

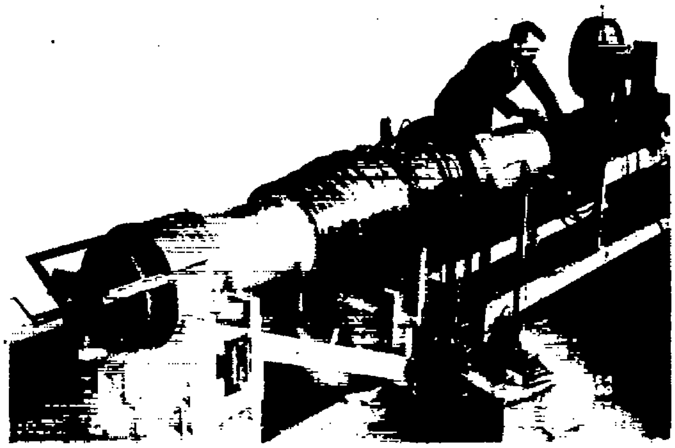

FIGURE 2.—View of axial-fan arrangement from exit end.

were made at various times during the tests. Any variation in the no-load torque, caused possibly by changes in bearing friction, was allowed for in the data. The torque coefficients include the torque necessary to rotate the hub as well as the blades.

The electric motor, which supports the fan hub and blades on its shaft, is mounted inside the fan casing by four streamline struts. Each strut contains four orifices on each side, which were used for measuring the quantity of air flowing. The pressure difference between these orifices and the atmosphere was calibrated against quantity of air flow. A venturi tube was used for this calibration.

The casing of the fan was of rolled and welded steel plate, bored to a diameter of 21 inches and relieved to

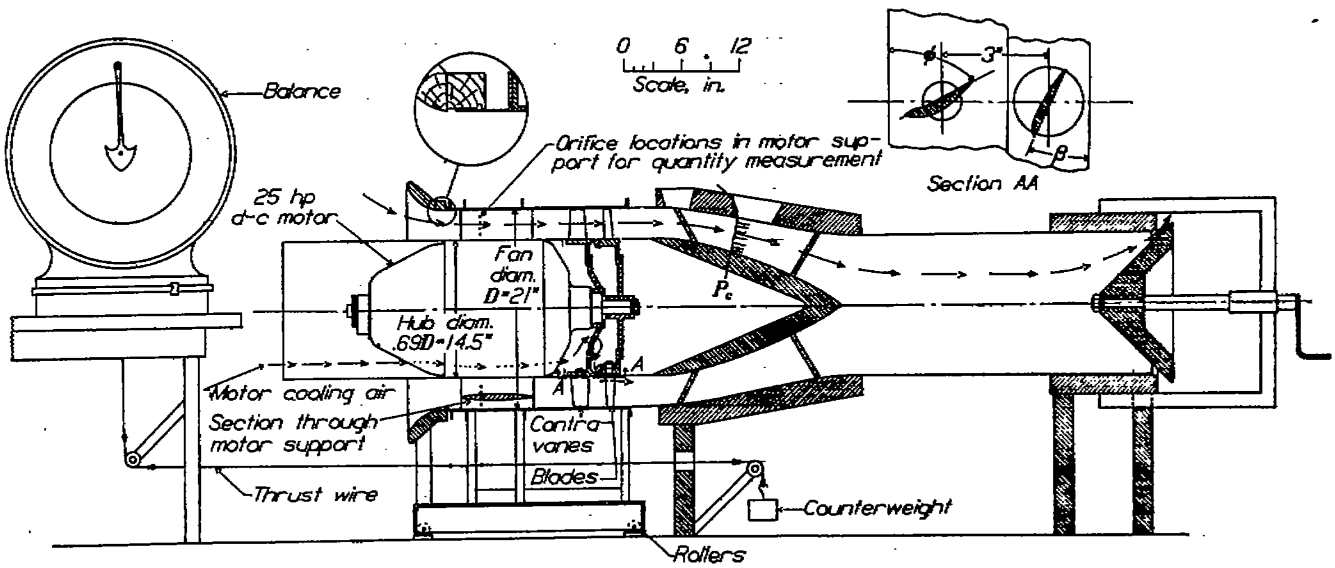

FIGURE 3.—Axial-fan test arrangement.

blade has a straight twist of 2° per inch of blade length and is not tapered. The blades were cut from solid bar stock duralumin on a profiling machine and were polished and buffed by hand.

Figure 6 shows the contravanes and the fixed hub assembly. Thirty-seven contravanes with a solidity of 1.33 were used. Figure 7 is a sketch of an individual contravane. The contravane airfoil section was arrived at by laying out an arbitrary camber line and using an NACA 0012 thickness distribution. The ordinates of the resulting section are given in figure 7. The contravanes were twisted 3° per inch of length and were not tapered. The spacing between blade and contravane center lines was 3 inches. A small clearance between the blade hub and the contravane hub allowed a slight amount of cooling air to flow through the motor.

The power for the fan is supplied by a 25-horsepower, direct-current electric motor. Before it was mounted in the fan casing, the motor was calibrated with a Prony brake for torque output as a function of armature current at a constant value of field current. No-load runs with the fan rotor assembly (fig. 4) removed

a diameter of $21\frac{1}{16}$ inches at the fan section. The contravanes were mounted in a hub that was carried on the motor frame. The fan casing was carried by a steel framework on a welded angle-iron base, which was in turn mounted on rollers resting on hardened and ground steel tracks. The rollers provided a means of measuring the thrust produced by the fan. The entrance cone for the fan was separately supported, as shown in the auxiliary view of figure 3. There was

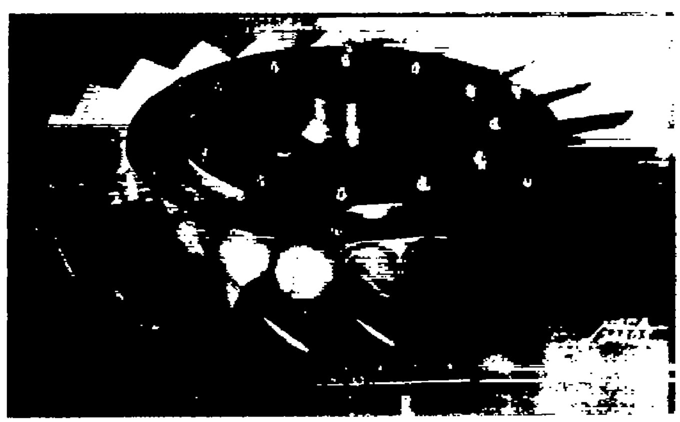

FIGURE 4.—Axial-fan blade wheel.

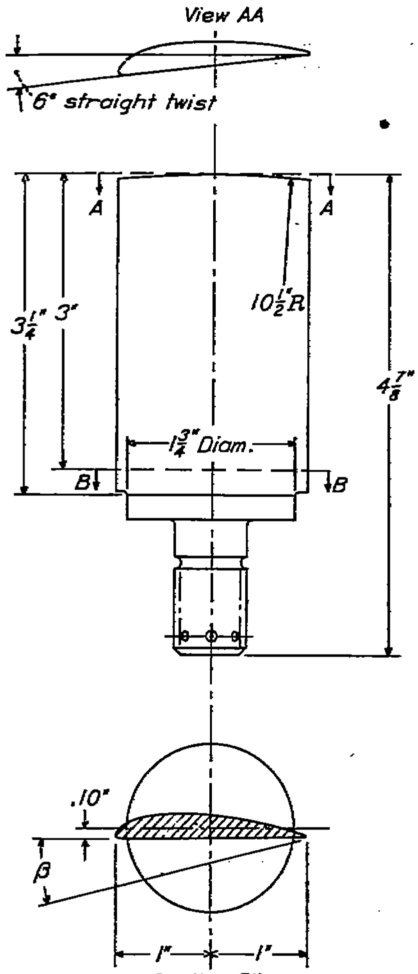

Section BB
FIGURE 5.—Axial-fan blade.

B. A. F. 6 (12 percent) propeller section	
Station	Ordinate
0	0
.050	.0985
.100	.142
.200	.1895
.400	.2280
.600	.240
.800	.2385
1.000	.228
1.200	.209
1.400	.1775
1.600	.1345
1.800	.084
2.000	0
L. E. radius	.024
T. E. radius	.019

FIGURE 6.—Axial-fan contravane wheel.

a close but free joint between the entrance cone and the fan casing. A cylinder having a diameter equal to that of the hub and motor was projected upstream into the free air far enough to extend beyond the pressure field of the entrance. The exit cones were independently supported and were separated from the fan by an air gap. The working section of the fan was therefore free to roll fore and aft on its rollers to a limited extent. Connected to the supporting framework and parallel to the thrust axis was a thrust wire. One end of the thrust wire was carried over a pulley and

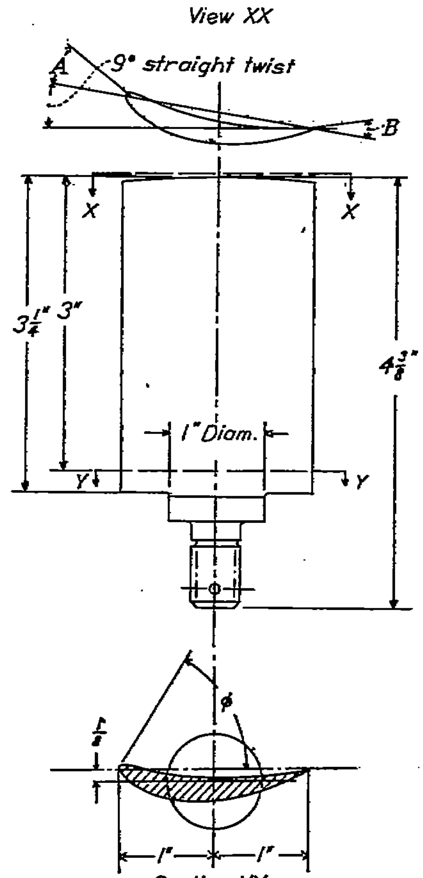

Section YY
FIGURE 7.—Axial-fan contravane.

Contravane section		
Station	Upper ordinate	Lower ordinate
0	0	0
.025	.073	−.017
.050	.100	−.018
.100	.142	−.015
.150	.178	−.007
.200	.207	.003
.300	.253	.027
.400	.288	.049
.500	.312	.068
.600	.325	.083
.800	.335	.104
1.000	.324	.111
1.200	.292	.107
1.400	.242	.091
1.600	.175	.066
1.800	.095	.032
1.900	.050	.015
2.000	0	0
L. E. radius	0.032	
T. E. radius	.0025	
A	30°	
B	19°	

connected to a dial-balance head. The other end of the thrust wire was carried over a pulley and connected to a weight pan. The dial balance and all counterweights used were carefully calibrated before the tests were made.

The exit cone was provided with a celluloid window through which tufts, located in the air stream, could be viewed for the purpose of estimating the stream twist angle. At the downstream end of the set-up a conical plug mounted on a screw thread was used for varying the restriction and controlling the volume of flow.

On the end of the motor, opposite the fan hub, was mounted the generator of a Weston tachometer. This instrument was wired to a milliammeter, the reading of which was frequently calibrated against motor speed.

DESCRIPTION OF TESTS

All tests were run at a speed of 3600 rpm except in cases in which the torque would have exceeded 36.5 foot-pounds, which corresponded to the motor rating. Under those conditions the tests were run at maximum motor torque.

A series of tests was run with several contravane-angle settings ranging from 40° to 70° and another series was run without contravanes. At each of these conditions the blade angles were varied from 5° or 10° to 35° or 40°. The quantity and the pressure coefficients were varied by changing the restriction at the outlet of the test set-up. At each point, data were taken of balance reading, amount of counterweight, manometer readings of the static pressure p_c and of the pressure at the orifices in the motor support, barometer reading, temperature, hygrometer reading, tachometer reading, motor field current, and motor armature current. The angle of flow downstream of the fan was estimated by looking at the tufts.

Extreme care was taken in setting the blade and the contravane angles but, because of the difficulty in setting them, they may not have been set closer than $\pm\frac{1}{4}°$. Blade and contravane angles were measured at a radius of $7\frac{1}{2}$ inches (71.4 percent R). Both blade and contravane angles were measured with respect to the same reference plane, that is, the plane of rotation of the blades.

PRESENTATION AND DISCUSSION OF RESULTS

The results of the test reported in this paper are presented in a manner similar to that used for propellers. Nondimensional coefficients, which are applicable to any similar axial fan operating at or near the same Reynolds and Mach numbers, are used.

$$C_T=\frac{T}{\rho n^2D^5} \text{ torque coefficient}$$

$$C_p=\frac{\Delta p}{\rho n^2D^2} \text{ pressure coefficient}$$

$$\eta=\frac{1}{2\pi}\frac{C_p}{C_T}\frac{Q}{nD^3} \text{ efficiency}$$

These coefficients are plotted against the quantity coefficient Q/nD^3

where:

- D fan diameter, 1.75 feet
- n rotational speed, revolutions per second
- Δp pressure rise across fan, pounds per square foot
- Q quantity rate of flow, cubic feet per second
- ρ mass density of air, slugs per cubic foot
- T torque, foot-pounds

also:

- p_c static pressure on downstream side of fan hub
- β blade angle, degrees
- ϕ contravane angle, degrees
- ψ stream twist angle, degrees
- R blade radius

The coefficient Q/nD^3 corresponds to V/nD as used for propellers and is also proportional to the discharge coefficient φ as used in reference 1. For the particular fan tested $Q/nD^3=0.412\ V/nD$ (where V=average velocity through the disk) and $Q/nD^3=1.29\varphi$.

The pressure rise across the fan was taken as the thrust on the disk area divided by the disk area. The thrust on the disk area is equal to the thrust obtained on the thrust system (balance and counterweights) corrected for the force resulting from pressure on the downstream side of the hub, that is, p_c measured in the space inside the exit cone. This correction was either added to or subtracted from the thrust, depending on whether p_c was below or above atmospheric pressure. As the horizontal areas at the free joints on either end of the blower outer casing were small, the correction for any pressure difference at these points was neglected. No correction was made for any pressure drop due to flow of cooling air.

The coefficient C_p is proportional to the pressure coefficient used in reference 1, which in the notation of this paper is $\Delta p/\frac{\rho}{2}u^2$, where u is the rotational tip speed. For this fan, $C_p=4.93\ \Delta p/\frac{\rho}{2}u^2$.

The results are presented in figures 8 to 28 as follows:

Figures:	Contravane-angle setting, ϕ (deg)
8 to 11	40.
12 to 15	50.
16 to 19	60.
20 to 23	70.
24 to 27	No contravanes.
28	Variation of fan characteristics with rotational speed.

Two plots of the pressure-coefficient data are presented. In one plot, the test points are given and lines of constant angle of twist downstream from the fan are superimposed. In the other plot, lines of constant efficiency are superimposed to facilitate design work.

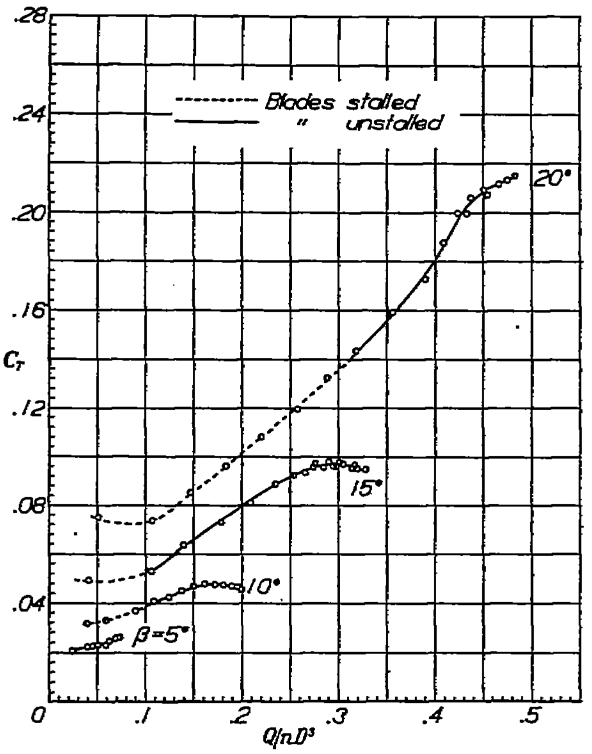

FIGURE 8.—Torque coefficients. ϕ, 40°.

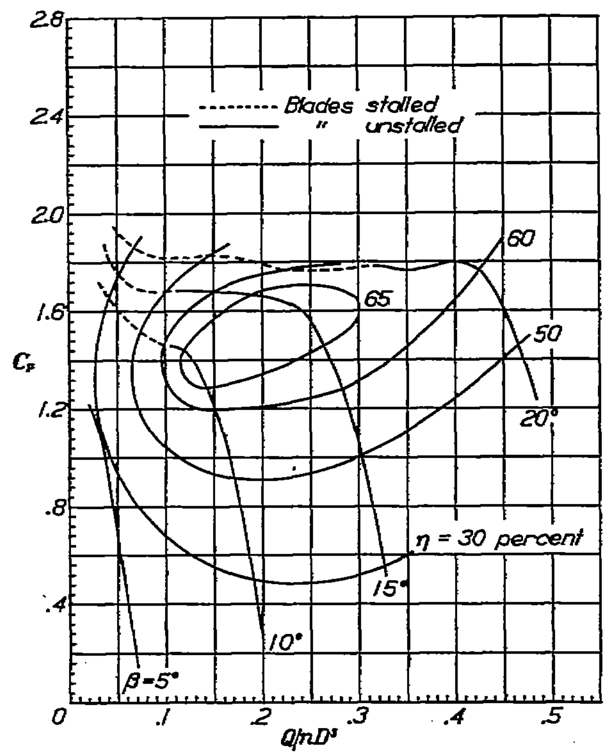

FIGURE 10.—Pressure coefficients showing lines of constant efficiency. ϕ, 40°.

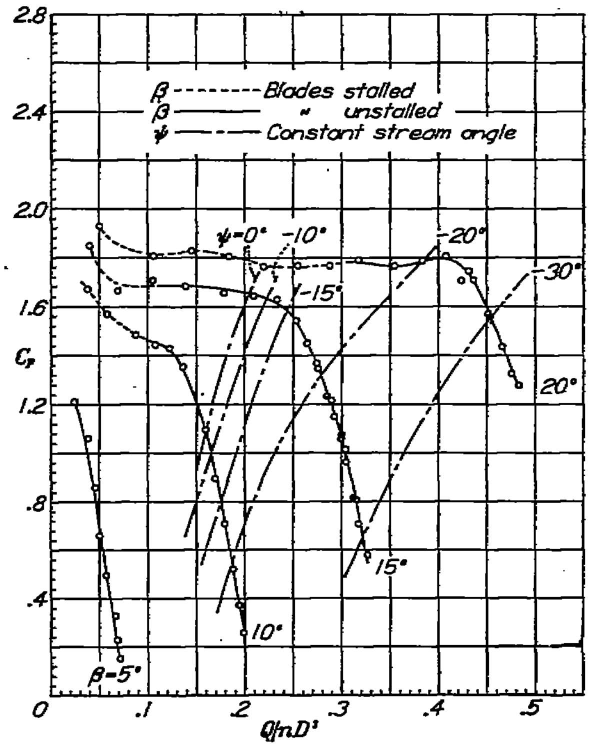

FIGURE 9.—Pressure coefficients. ϕ, 40°.

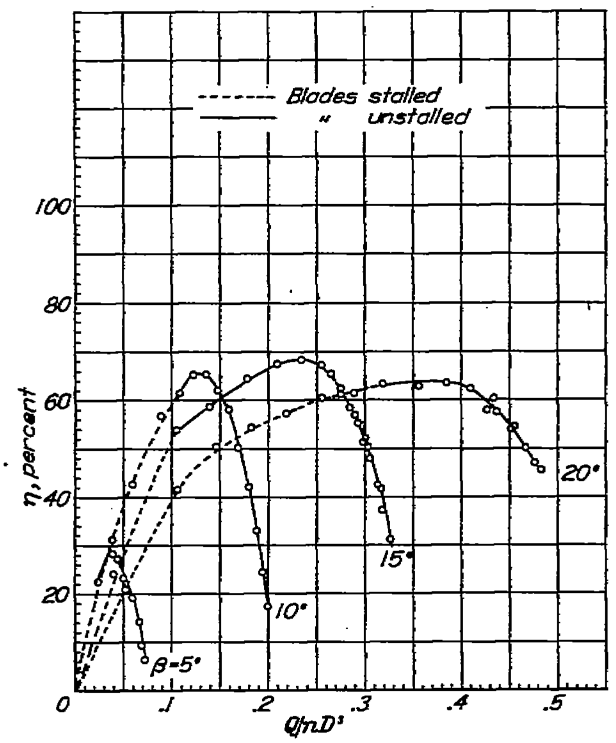

FIGURE 11.—Axial-fan efficiencies. ϕ, 40°.

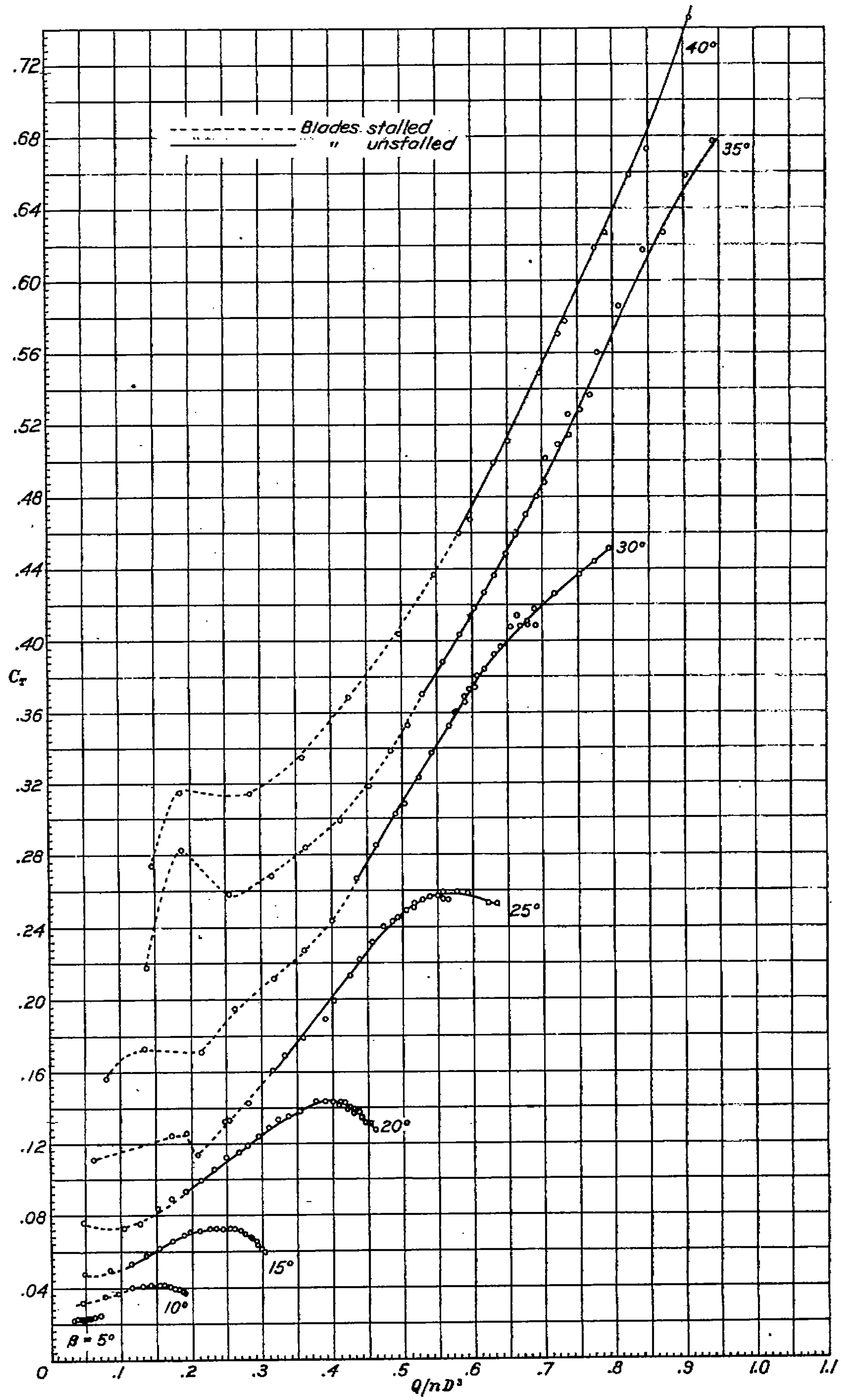

FIGURE 12.—Torque coefficients. φ, 50°.

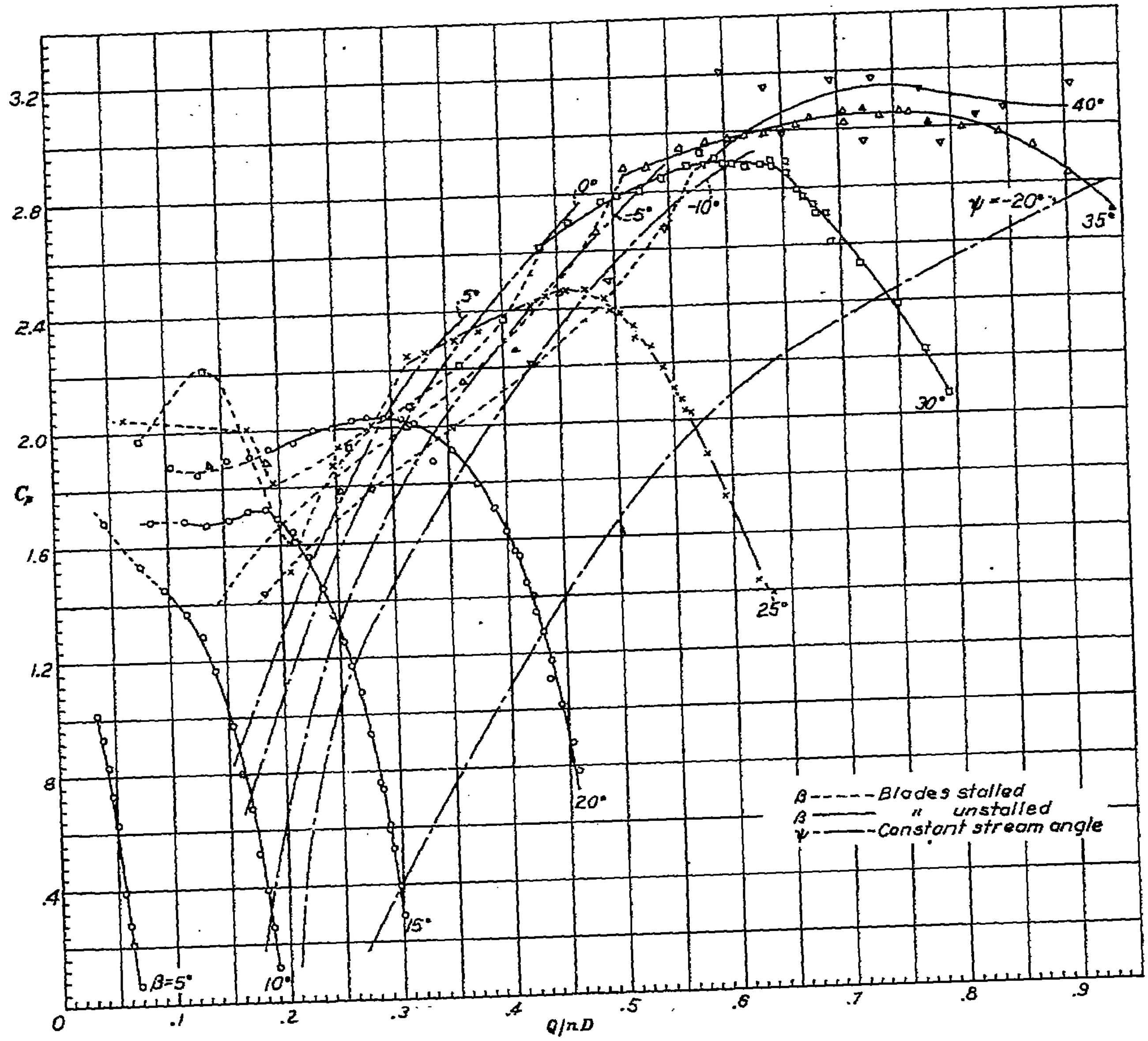

FIGURE 13.—Pressure coefficients. ϕ, 50°.

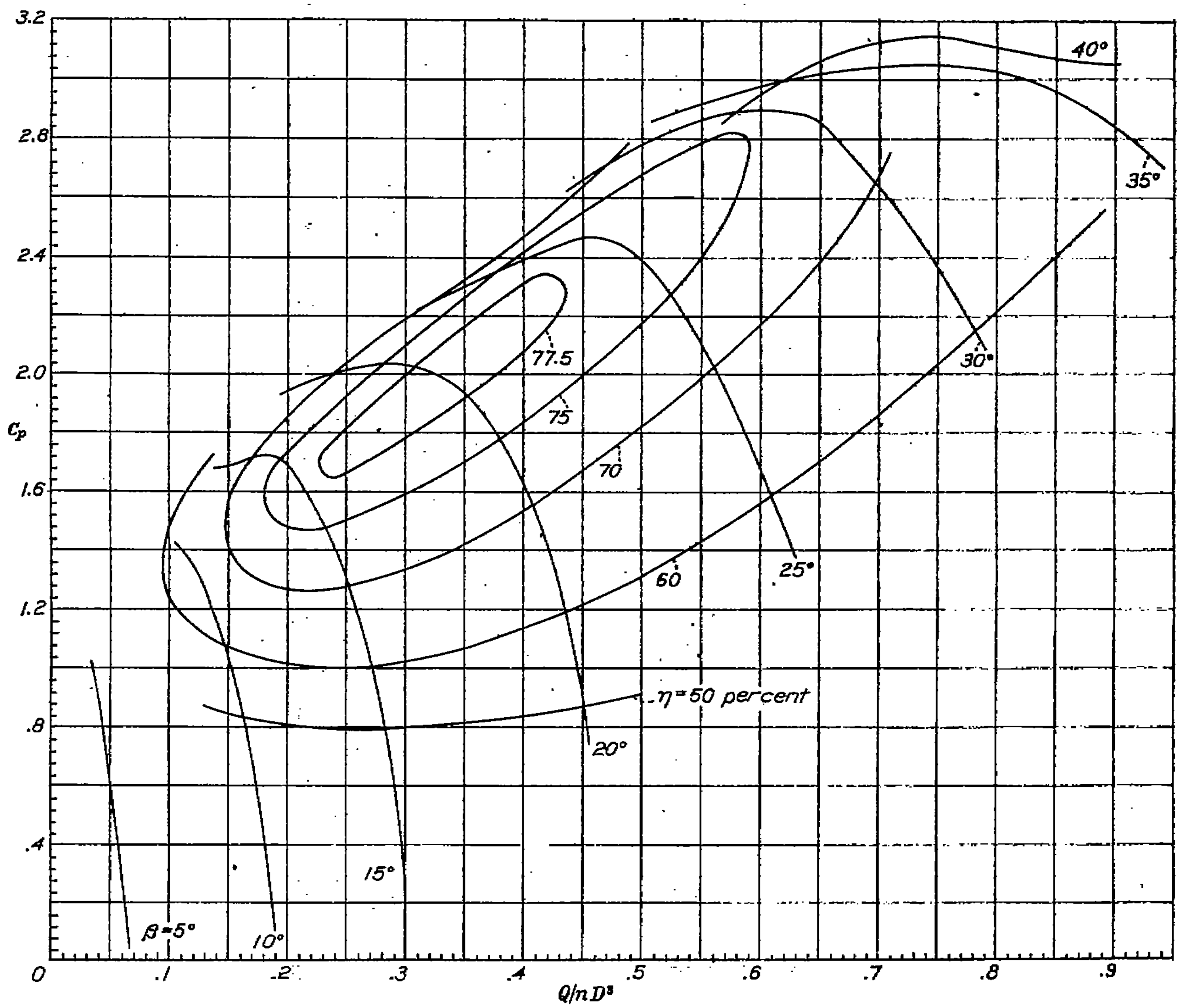

FIGURE 14.—Pressure coefficients showing lines of constant efficiency. φ, 50°.

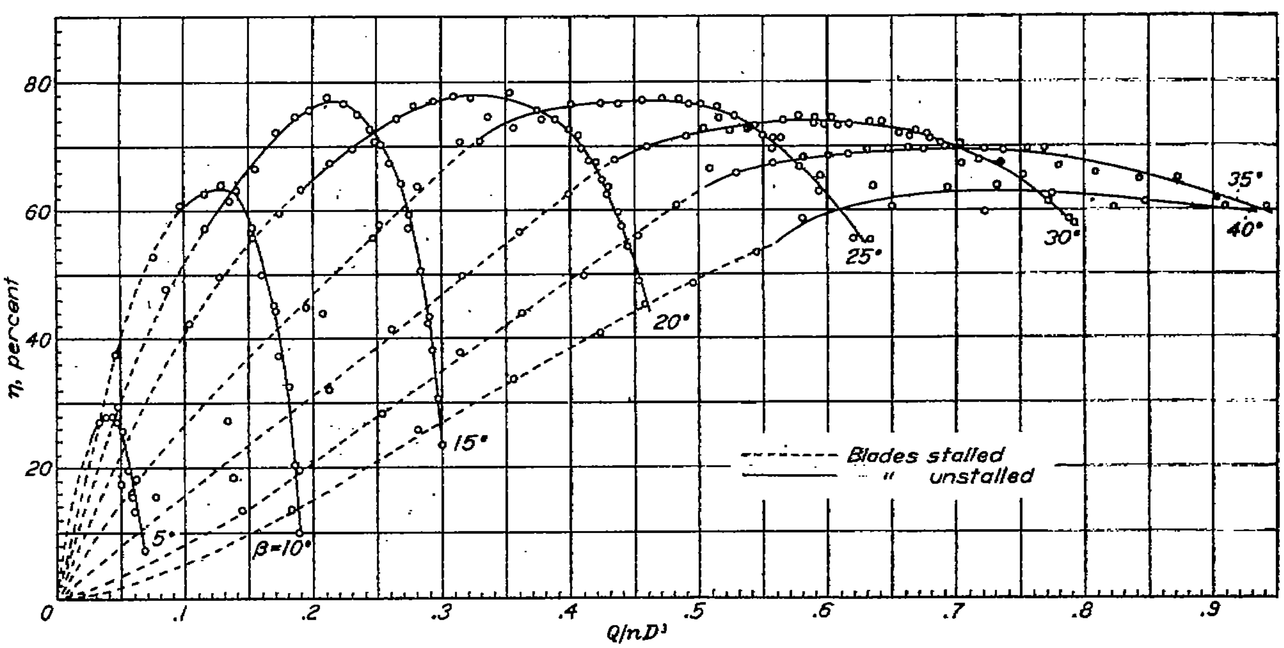

FIGURE 15.—Axial-fan efficiencies. φ, 50°.

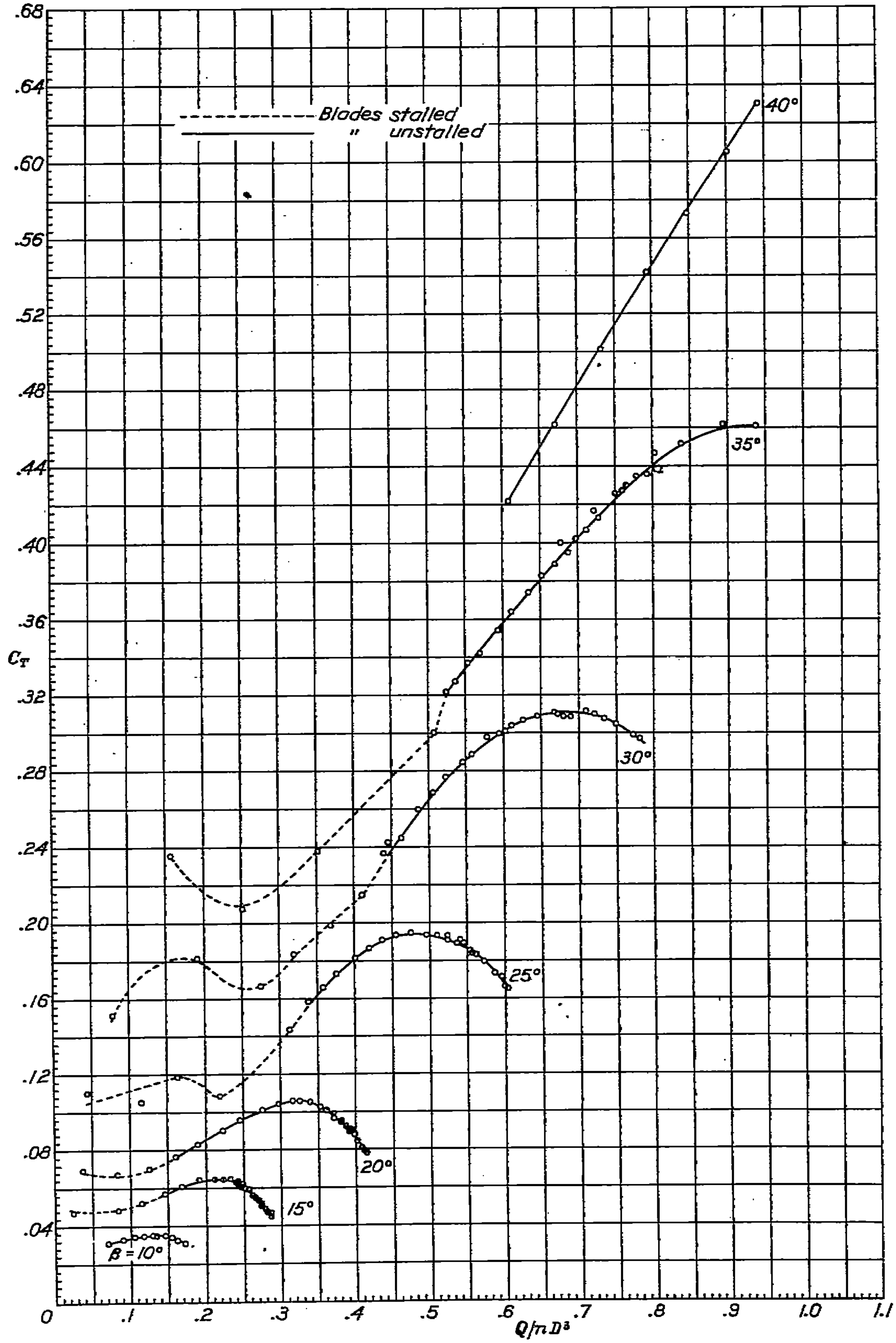

FIGURE 16.—Torque coefficients. ϕ, 60°

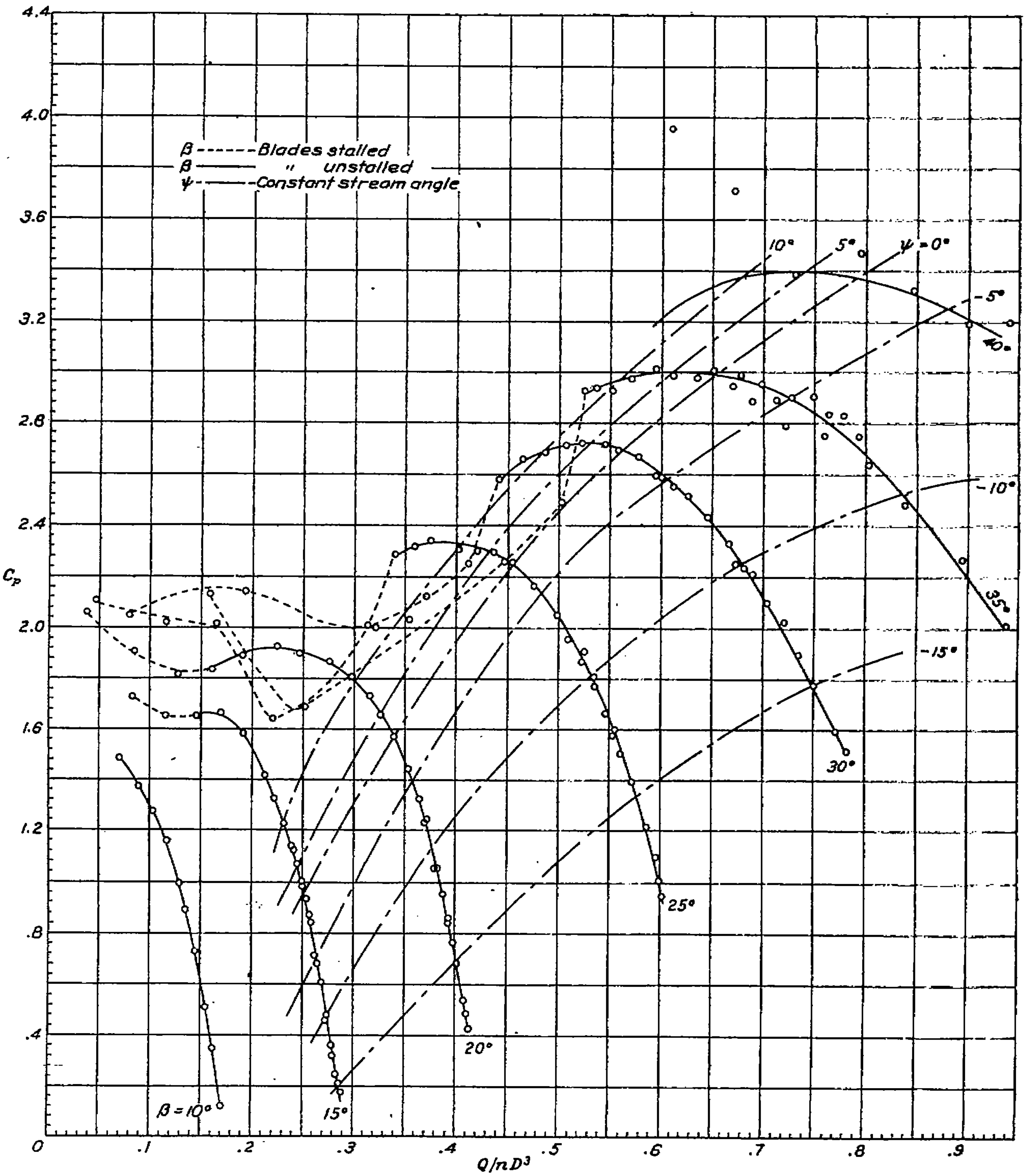

FIGURE 17.—Pressure coefficients. ϕ, 60°.

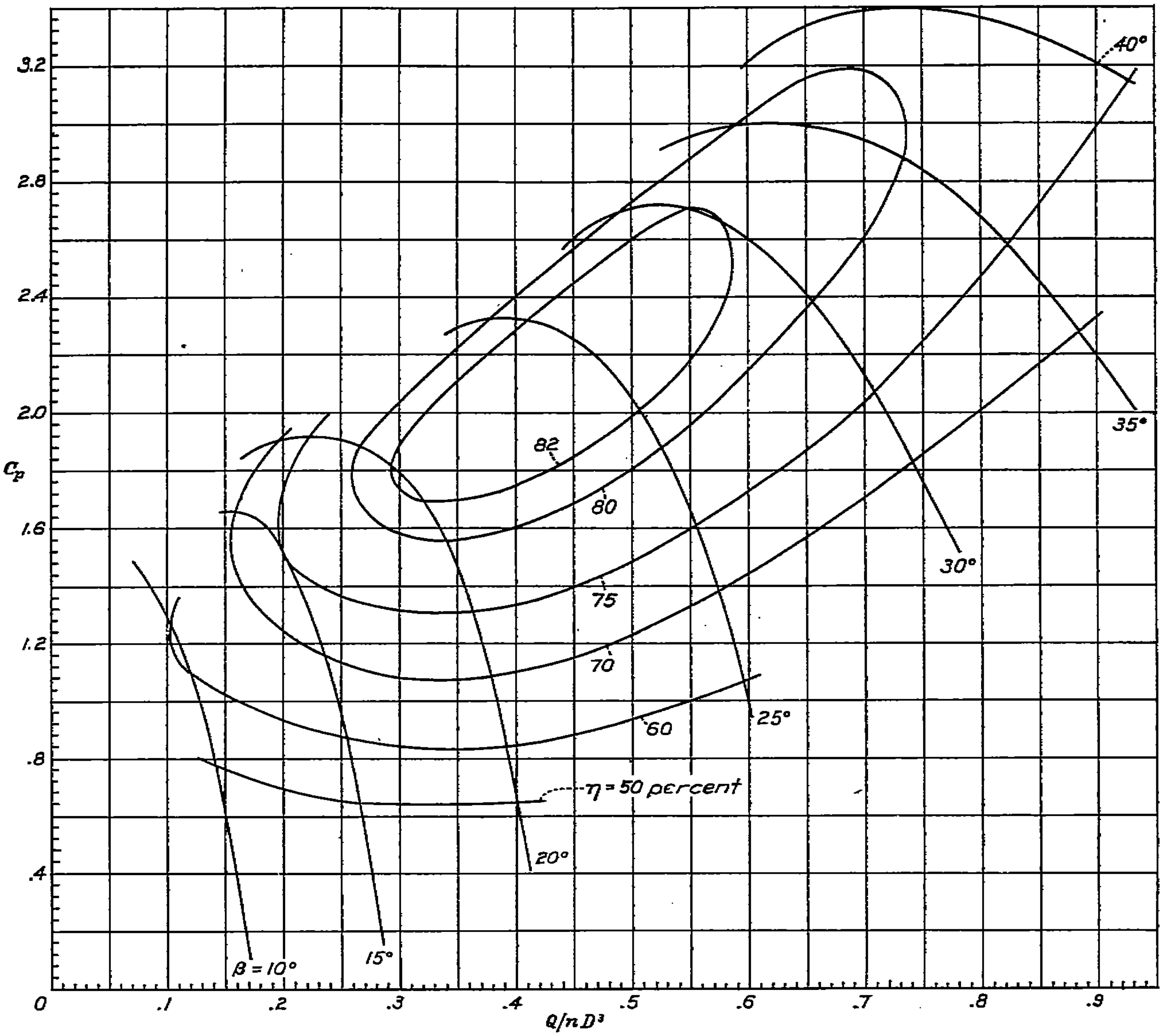

FIGURE 18.—Pressure coefficients showing lines of constant efficiency. ϕ, 60°.

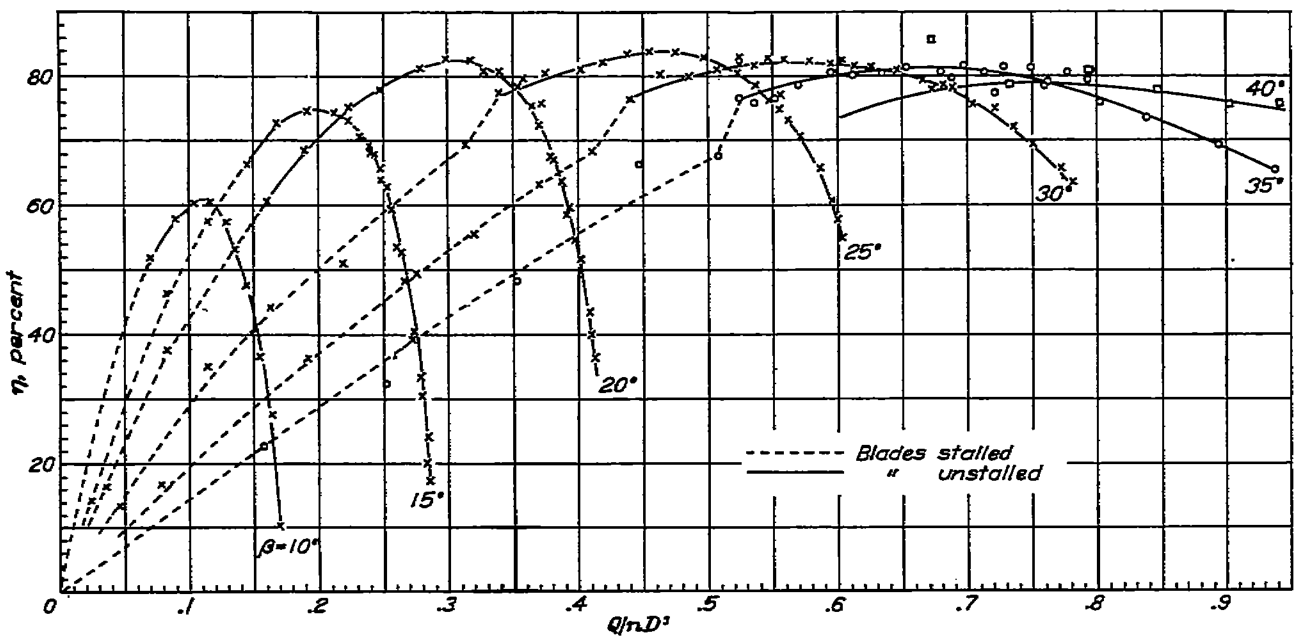

FIGURE 19.—Axial-fan efficiencies. ϕ, 60°.

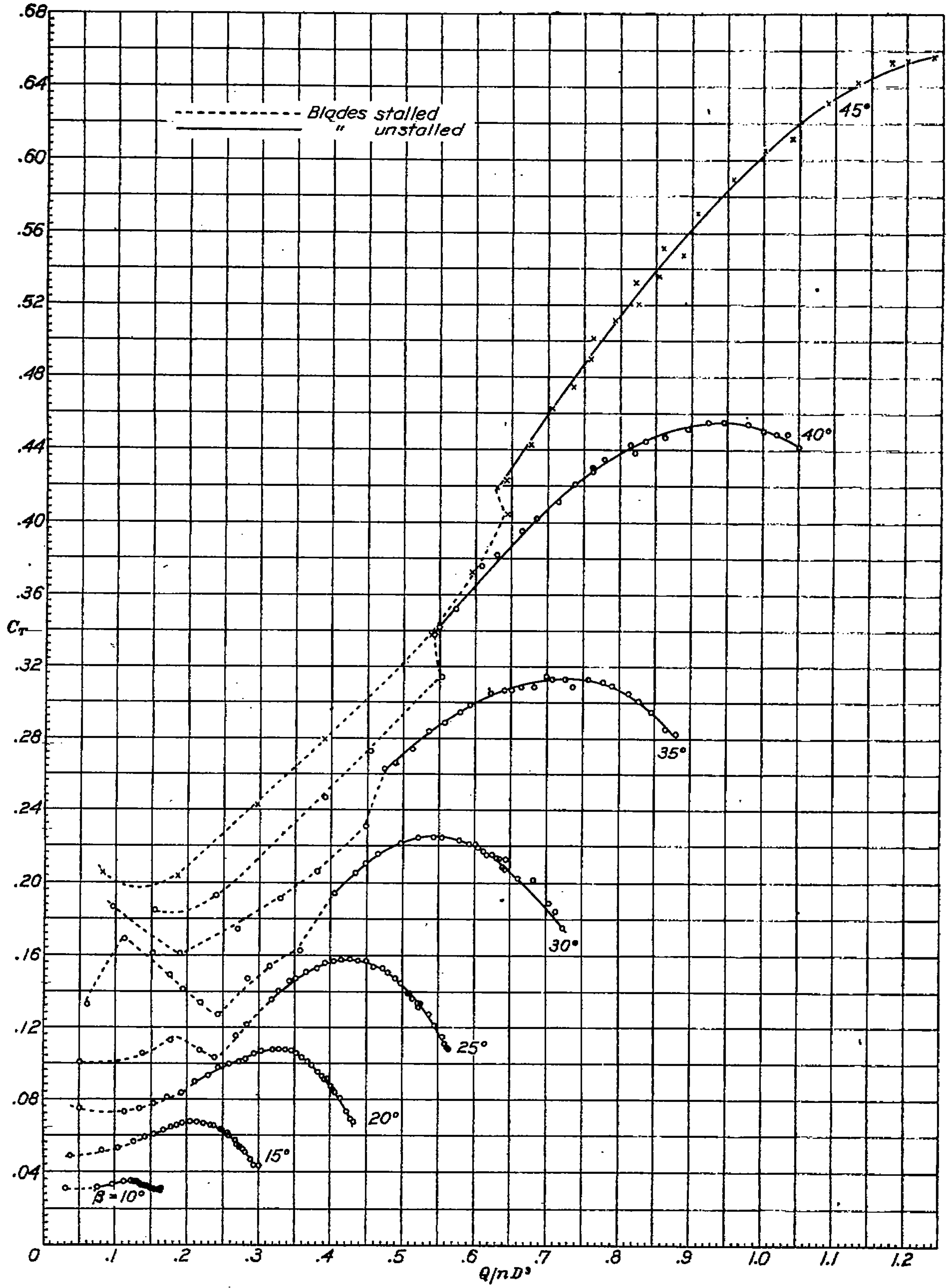

FIGURE 20.—Torque coefficients. φ, 70°.

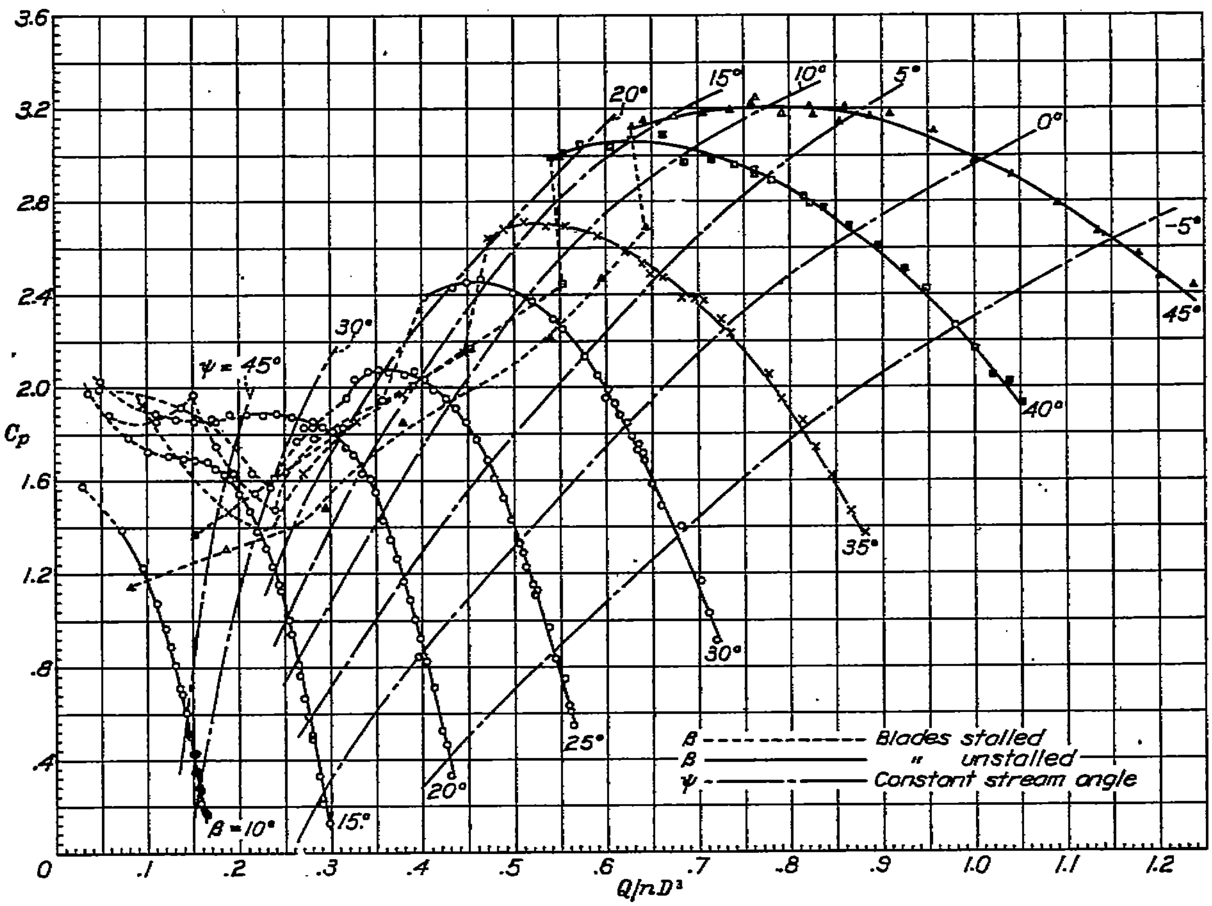

FIGURE 21.- Pressure coefficients. ϕ, 70°.

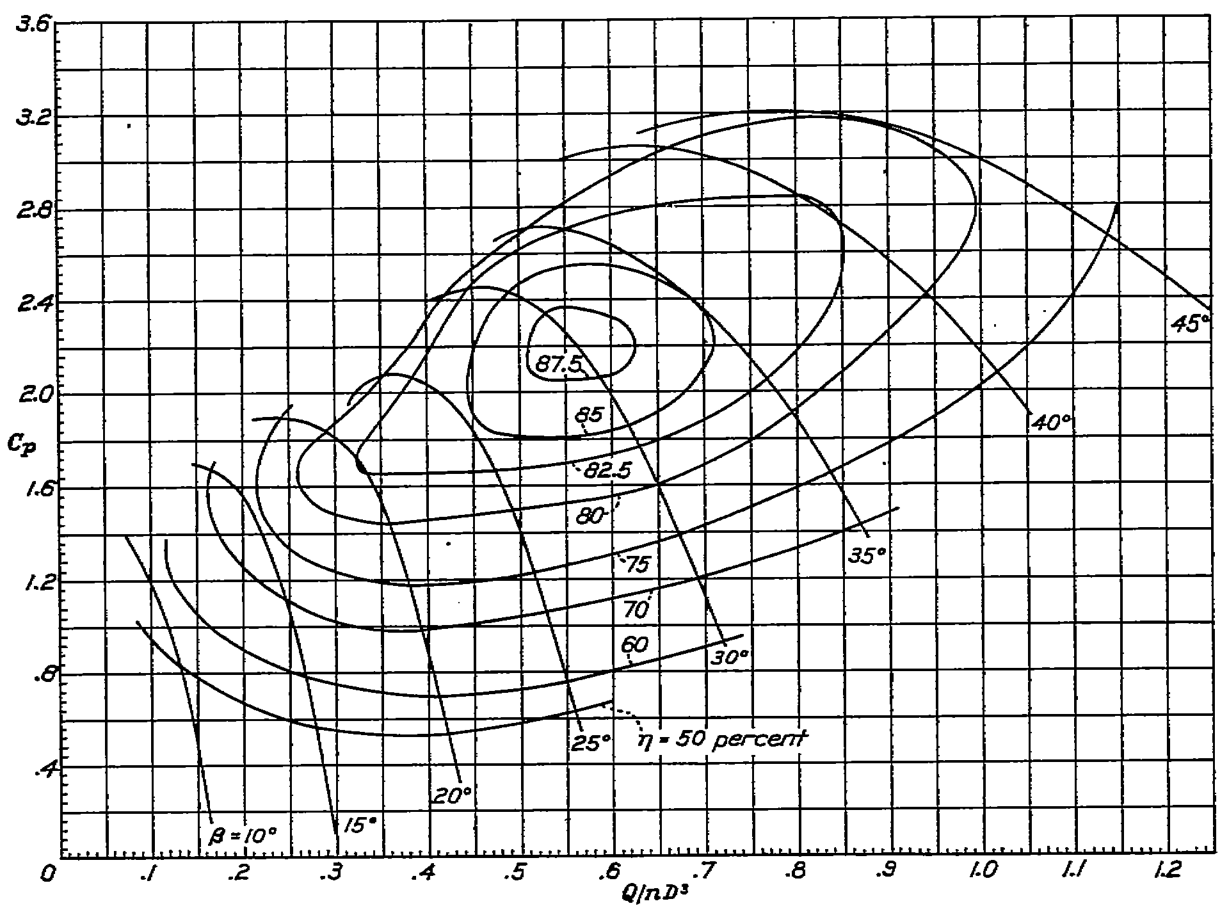

FIGURE 22.—Pressure coefficients showing lines of constant efficiency. ϕ, 70°.

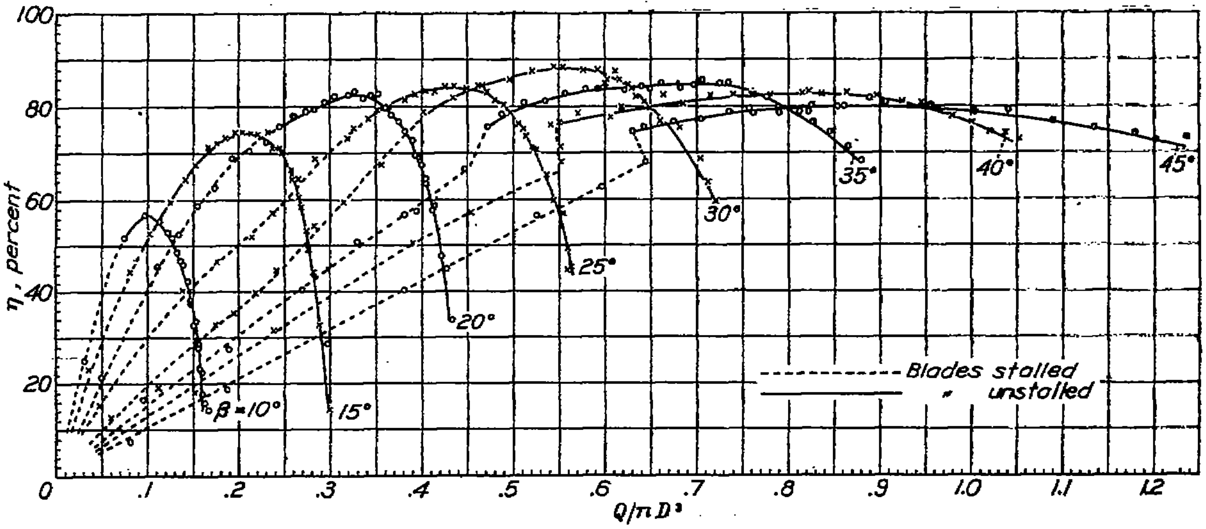

FIGURE 23.—Axial-fan efficiencies. φ, 70°.

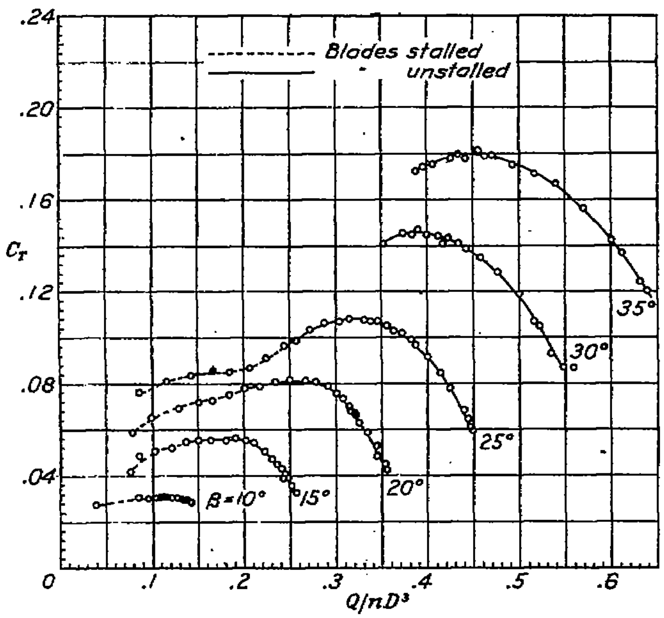

FIGURE 24.—Torque coefficients. No contravanes.

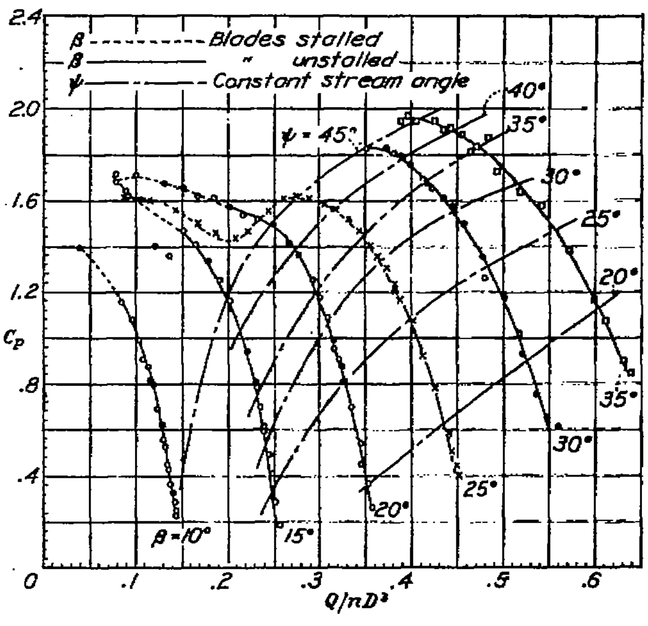

FIGURE 25.—Pressure coefficients. No contravanes.

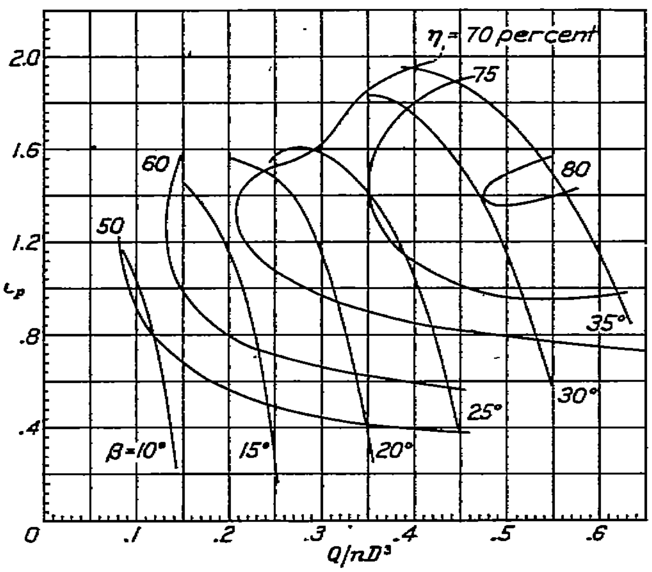

FIGURE 26.—Pressure coefficients showing lines of constant efficiency. No contravanes.

The stream angle ψ, for which constant values are imposed on the pressure-coefficient plots in figures 9, 13, 17, 21, and 25, is the average stream angle as estimated by viewing the tufts located behind the blade wheel. Under certain conditions there was considerable variation of the angle along the radius. It is believed, however, that the stream angle of most of the air was within $\pm 3°$ of that given. Positive values of ψ indicate that the air steram was twisting in the direction of rotation of the rotor.

The maximum efficiency of 88 percent for this fan was found to be at a blade-angle setting of 30° and a contravane setting of 70°. It is interesting to note that the contravane setting of 70° yielded the highest efficiencies for nearly all values of Q/nD^3.

The fan efficiency with contravanes removed was 80 percent as compared with 88 percent with the contravanes set 70°. This loss of 8 percent results from the

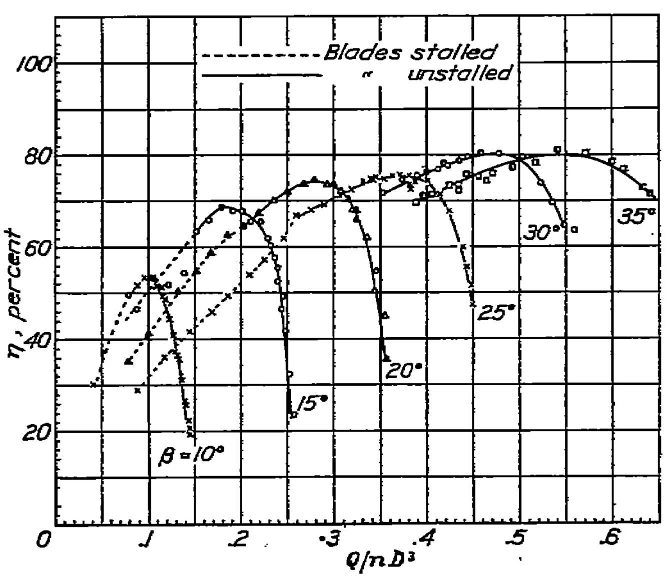

FIGURE 27.—Axial-fan efficiencies. No contravanes.

fact that the rotational losses occurring without contravanes were greater than the profile drag of the contravanes. The downstream angle of twist for the peak-efficiency condition with contravanes set 70° was about 5° or 10°, whereas the angle of twist with contravanes removed was about 25°.

Of perhaps more importance than the effect on efficiency is the effect of contravanes on the pressures produced. The maximum pressures for a given quantity of flow were found to be considerably less with contravanes removed than with them installed, regardless of the blade-angle setting. When the contravanes

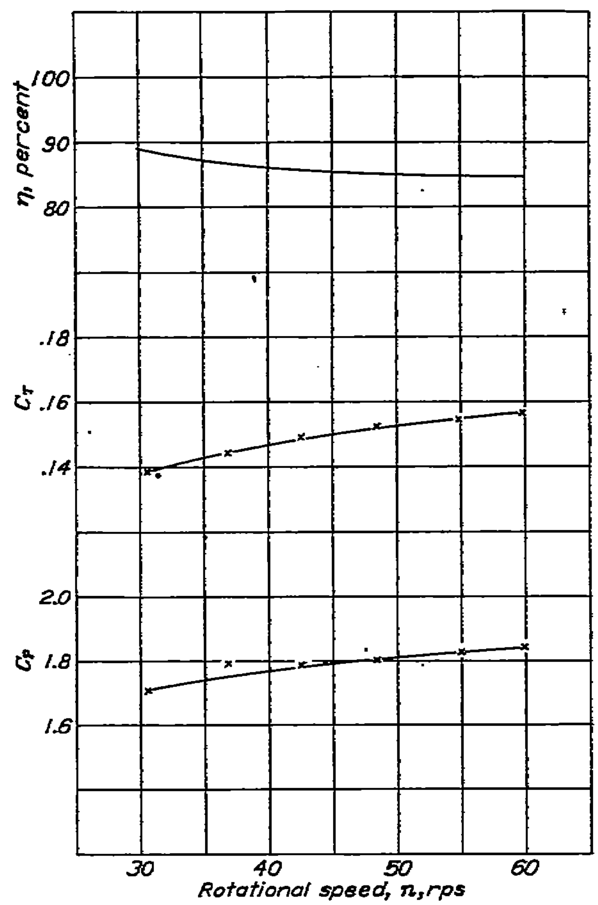

FIGURE 28.—Variation of fan characteristics with rotational speed. Q/nD^3, 0.45; β, 25°; ϕ, 70°.

were removed, the rotational interference velocity was in the same direction as the blade rotational velocity. The result was a certain relative velocity over the blade surfaces and, consequently, a certain pressure. When the contravanes were in place, the air was given an inflow rotational-velocity component opposite in direction to that of the rotor, the result being an increase in the relative velocity between the air and the rotor blades and an increase in pressure.

The stalling characteristics of the fan were very pronounced. As long as the blades were unstalled, operation was very smooth. As the restriction was increased and the flow was decreased, however, the fan reached a stalling point beyond which the operation became very rough and noisy. In some cases the quantity of air flow dropped off considerably with stalling, and it was impossible to obtain points for a curve. On all the curves, the stalled portion is indicated by dotted lines when enough points could be obtained to justify it. It is recommended, however, that fans be designed to operate only in the unstalled portion.

As the range of this fan was limited by both the torque and the speed characteristics of the motor, little attempt was made to get an extensive evaluation of scale effect. One series of tests was made, however, at $\beta=25°$ and $\phi=70°$ for a short range of Q/nD^3 at different blower speeds. Values of C_T, C_p, and η were taken from these tests at a value of $Q/nD^3=0.45$. These values are plotted in figure 28 against fan rotational speed, and the results indicate that, while the pressure and the torque increase, the efficiency decreases with Reynolds number. The variation of pressure and torque coefficients with Reynolds number is unexpectedly large.

No effects from compressibility would be expected from these tests, inasmuch as the highest tip speed was only 330 feet per second. Compressibility should be taken into account for designs wherein the tip speeds will be above 600 feet per second.

LANGLEY MEMORIAL AERONAUTICAL LABORATORY,
NATIONAL ADVISORY COMMITTEE FOR AERONAUTICS,
LANGLEY FIELD, VA., *September 22, 1941.*

REFERENCE

1. Keller, Curt, Marks, Lionel S., and Weske, John R.: The Theory and Performance of Axial-Flow Fans. McGraw-Hill Book Co., Inc., 1937.